Increased sensitivity of higher-order laser beams to mode mismatches

Jones, A. W.; Freise, A.

published in
Optics Letters
2020

DOI (link to publisher)
10.1364/OL.403802

document version
Publisher's PDF, also known as Version of record

document license
Article 25fa Dutch Copyright Act

Optics Letters

Increased sensitivity of higher-order laser beams to mode mismatches

A. W. Jones[1,2,*] and A. Freise[1,3,4]

[1]School of Physics and Astronomy and Institute for Gravitational Wave Astronomy, University of Birmingham, Edgbaston, Birmingham B15 2TT, UK
[2]OzGrav, University of Western Australia, Crawley, Western Australia, Australia
[3]Department of Physics and Astronomy, VU Amsterdam, De Boelelaan 1081, 1081, HV Amsterdam, The Netherlands
[4]Nikhef, Science Park 105, 1098, XG Amsterdam, The Netherlands
*Corresponding author: aaron.jones@ligo.org

Received 26 August 2020; revised 15 September 2020; accepted 18 September 2020; posted 18 September 2020 (Doc. ID 403802); published 15 October 2020

This Letter derives explicit factors linking mode-mismatch-induced power losses in Hermite–Gauss optical modes to the losses of the fundamental spatial mode. Higher-order modes are found to be more sensitive to beam parameter mismatches. This is particularly relevant for gravitational-wave detectors, where lasers employing higher-order optical modes have been proposed to mitigate thermal noise, and quantum-enhanced detectors are very susceptible to losses. This work should inform mode matching and squeezing requirements for Advanced+ and third generation detectors.

https://doi.org/10.1364/OL.403802

Optical higher-order modes (HOMs) have a wide range of uses, for example, driving micro-machines [1,2], manipulation of cold atoms [3], and telecommunications [4]. In precision metrology, the performance of current and future gravitational-wave detectors is limited by self-noise of the detectors, which is dominated over a wide frequency band by the quantum noise of the interrogating light field and the thermal noise of the optics. The introduction of non-classical light (also called *squeezing*) into advanced gravitational-wave detectors [5], leaves thermal noise as the fundamentally limiting noise in the detectors' most sensitive frequency range [6].

There are proposals to use a HOM as the carrier mode in the interferometer to mitigate thermal noise [7–9] in gravitational-wave detectors. This technique may also be of interest to other thermal-noise-limited optical cavities [10]. Sorazu *et al.* studied the use of a Laguerre–Gauss 3,3 (LG33) mode in a 10 m suspended optical resonator [11] and noted that astigmatism caused the break up of the LG33 mode into component Hermite–Gauss (HG) modes with a similar, but not equal, round trip Gouy phase, resulting in distorted control signals and a poor power coupling into the resonator.

Adaptive astigmatism control could be used to mitigate LG33 break-up [12]. Alternatively, HG modes are naturally astigmatic, and may be more compatible with the long baseline optical resonators used in gravitational-wave detectors [10]. The HG55 has been discussed [10] as a possible option. However, it is well known that the transfer of squeezed light into the interferometer is exceptionally sensitive to optical losses [13]. Mode mismatch can be a dominant source of squeezing loss [14] and a 98% mode-matching target is achievable with Advanced LIGO+, potentially allowing 8 dB of squeezing [15].

This Letter revisits the subject of HOM to resonator matching, in the context of HG modes, and derives an increased sensitivity to mode mismatch that scales monotonically with mode index. For the HG55, the losses due to waist-size mismatch would be 31 times worse than for the fundamental mode. Results for a waist position mismatch are shown in Supplement 1. Our results are derived using a computer algebra system [16] and shown to match numeric integration. A higher-order astigmatic beam passing though the LIGO Output Mode Cleaner (OMC) is considered as an example of applying these coefficients. These results are consistent with the evidence discussed in [11], the decreased mode purity and power observed in [10], and experimental observations in [17].

The mode-coupling coefficients were derived in the general case in 1984 by Bayer–Helms [18]. Consider two mode bases, the first with waist w_0 at z_0 (typically the mode basis of the incoming light) and the second with waist $\bar{w}_0$ at $\bar{z}_0$ (typically the resonator mode basis). Then, the amplitude coupling of a mode with indices n, m in the first basis to mode $\bar{n}$, $\bar{m}$ in the second basis is described by $k_{n,m,\bar{n},\bar{m}}$, which is in general complex. In this work, all parameters with an overline correspond to the resonator basis.

For HG modes, this coupling coefficient is separable [18]:

$$k_{n,m,\bar{n},\bar{m}} = k_{n,\bar{n}} k_{m,\bar{m}}. \tag{1}$$

If the beam axis is aligned, then the 1D coupling coefficients are reduced to [18]

$$k_{n,\bar{n}} = \int_{-\infty}^{\infty} u_n(x', z)\, \bar{u}_{\bar{n}}^*(x', z)\, \mathrm{d}x'. \tag{2}$$

Considering only $w_0 \neq \bar{w}_0$, $z_0 = \bar{z}_0$ (see Supplement 1 for $w_0 = \bar{w}_0$, $z_0 \neq \bar{z}_0$), then evaluating both beams at the waist

$z = z_0$, the beam size is $w(z) = w_0$, and the radius of curvature is $R_C = \infty$. Additionally, the Gouy phase of the resonator mode at the waist is zero $\bar{\Psi}(z_0) = 0$. Then, by rescaling $x = x'/\bar{w}_0$, the spatial properties of the resonator eigenmodes are [19]

$$\bar{u}_{\bar{n}}(x, z) = \left(\frac{2}{\pi}\right)^{\frac{1}{4}} \sqrt{\frac{1}{2^{\bar{n}}\bar{n}!}} H_{\bar{n}}(\sqrt{2}x) e^{-x^2}. \quad (3)$$

Defining the fractional waist-size mismatch, $w \equiv w_0/\bar{w}_0$, the distribution of the incoming light is

$$u_n(x, z) = \left(\frac{2}{\pi}\right)^{\frac{1}{4}} \sqrt{\frac{1}{2^n n! w}} \exp\left(\frac{i(2n+1)\Psi(z)}{2}\right) \times H_n\left(\frac{\sqrt{2}x}{w}\right) \exp\left(\frac{-x^2}{w^2}\right), \quad (4)$$

where Ψ is free to describe some accumulated Gouy phase. After substitution of Eqs. (4) and (3), Eq. (2) is difficult to solve. However, the integrate function from SymPy [16] v1.3, can solve this for a specific n, which may then be expanded with the series method. For the first 10 orders, the coupling constant between the same mode in each basis ($n = \bar{n}$) is

$$k_{n,n} \approx \exp\left(\frac{i(2n+1)\Psi(z)}{2}\right) \times \left(1 - \frac{C_n}{4}\left((w-1)^2 - (w-1)^3\right) + \mathcal{O}\left((w-1)^4\right)\right), \quad (5)$$

where

$$C_0 = 1, \quad C_1 = 3, \quad C_2 = 7, \quad C_3 = 13, \quad C_4 = 21, \quad C_5 = 31, \quad C_6 = 43, \quad C_7 = 57, \quad C_8 = 73, \quad C_9 = 91, \quad C_{10} = 111, \quad (6)$$

and Code 1, Ref. [20] can be used to compute additional values of C_n. Figure 1 shows a numerical solution to Eq. (2) using PyKat [21] against Eq. (5) expanded to order $(w-1)^3$. For a waist-size mismatch less than 5%, there is good agreement between the analytic solution and the numerical ones.

When considering a resonator, the power coupling efficiency, $k_{n,\bar{n},m,\bar{m}} k^*_{n,\bar{n},m,\bar{m}}$, is considered. Defining the horizontal losses to be

$$W_x \equiv \frac{(w-1)^2 - (w-1)^3}{4} \approx 1 - |k_{0,0}| \quad (7)$$

and likewise for the vertical losses, W_y, the full 2D coupling coefficient is

$$k_{n,n,m,m} \approx e^{i(n+m+1)\Psi(z)}(1 - C_n W_x - C_m W_y + C_n C_m W_x W_y). \quad (8)$$

For an almost matched beam in x and y, the last term may be safely ignored. The power coupling coefficient is then

$$k_{n,n,m,m} k^*_{n,n,m,m} \approx 1 - 2C_n W_x - 2C_m W_y, \quad (9)$$

where terms of orders W_x^2, W_y^2, and $W_x W_y$ have been neglected. This result conclusively shows that HOMs are more susceptible to mode mismatching losses when coupling into cavities.

Advanced LIGO operates with a high degree of mode matching to ensure power couples efficiently between the resonators; however, some degree of mismatch is always present.

Within the core interferometer, an increased sensitivity to mode mismatch will likely cause a reduced interferometric visibility. In addition, since the core interferometer is dual recycled and has focusing elements within the recycling cavities, an increased sensitivity to mode mismatch may lead to challenges in defining an operating point for the resonators [22].

In the case of the input mode cleaners (IMCs) and OMCs, modes that are not resonant are reflected and dumped. Therefore, the effect of the mode mismatch is a reduced power transmission through the resonator. In the case of the IMC, small mismatches can be compensated for by increasing laser power. In the case of the OMC, the mode mismatch directly causes a loss of signal and loss for squeezed light injection.

A Finesse model [23,24] of the Advanced LIGO OMC was produced, and the transmission efficiency was studied for a range of input modes; results are shown in Fig. 2. The input power was chosen such that a mode-matched beam produced 1 W of power on transmission, when the resonator was tuned and was constant for all simulations. This power scaling means that the power on transmission is equal to the OMC power coupling efficiency. The input beam was astigmatic with $w_{0x} = 0.98\bar{w}_{0x}$ and $w_{0y} = 0.96\bar{w}_{0y}$. This astigmatism was chosen to highlight the differing losses for modes with $m \neq n$. The tuning range was measured from the expected resonance

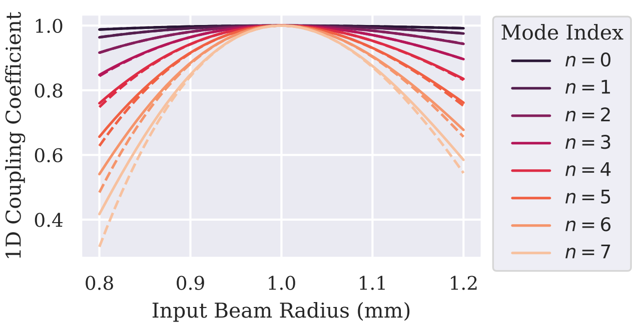

Fig. 1. 1D mode mismatch parameter, $k_{n,n}$ for a waist-size only mismatch between the incoming beam and the 1 mm resonator waist size. Solid lines show numerical solutions to Eq. (2), and dotted lines show the approximate analytic solutions in Eq. (5). See Supplement 1 for an analogous waist-position mismatch.

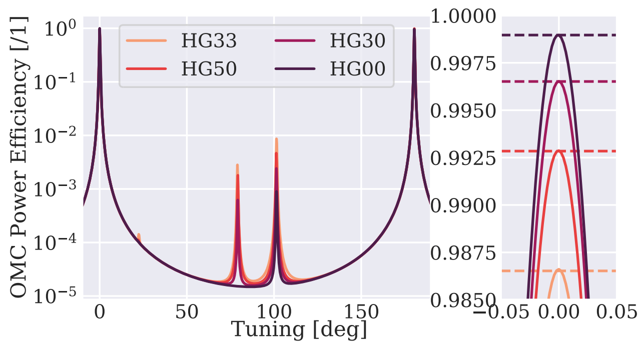

Fig. 2. Power transmitted by the Advanced LIGO OMC for an astigmatic input beam. On both plots, the x axis shows tuning from expected resonance position, and the y axis shows the transmitted power. The right-hand plot shows a zoom of the peak resonance on a linear scale, and dashed lines show efficiency determined with Eq. (11).

Table 1. Mode-Mismatch-Induced Power Losses through the OMC for an Astigmatic Input Beam[a]

Input Mode	Analytic (x)	Analytic (y)	Analytic (Total)	Simulation	Difference
HG00	204.0 ppm	832.6 ppm	1036.7 ppm	1036.5 ppm	0.2 ppm
HG30	2652.5 ppm	832.6 ppm	3485.1 ppm	3472.8 ppm	12.3 ppm
HG50	6325.1 ppm	832.6 ppm	7157.8 ppm	7131.6 ppm	26.1 ppm
HG33	2652.5 ppm	10824.1 ppm	13476.6 ppm	13389.8 ppm	86.8 ppm

[a]The analytic response is determined from Eq. (11), and the simulated response is determined from the Finesse cavity scan in Fig. 2.

position. Simulation modes n', m', up to $n' + m' \leq n + m + 4$, for input mode n, m were enabled.

The parameter $2W_x$ was determined by running an additional simulation with TEM00 input and $w_{0y} = \bar{w}_{0y}$ and $w_{0x} = 0.98\bar{w}_{0x}$; then

$$2W_x = 1 - \frac{P_{Tx}}{P_T}, \quad (10)$$

where P_{Tx} is the power measured on transmission, and P_T is the transmitted power for no mismatch. In this work, the input power scaling means $P_T = 1$. The parameter $2W_y$ was obtained similarly. The analytically determined OMC power coupling efficiency for mode HGnm is then

$$|k_{n,n,m,m}|^2 = 1 - C_n\left(1 - \frac{P_{Tx}}{P_T}\right) - C_m\left(1 - \frac{P_{Ty}}{P_T}\right), \quad (11)$$

which is shown by the dotted lines in Fig. 2. This general method also works as an experimental procedure and can be used to estimate losses in switching to a HOM.

$|k_{n,n,m,m}|^2$ was also obtained directly from the simulation by measuring the peak transmitted power, and a comparison is shown in Table 1. As an example, when the n index is increased from zero to three, the x related power losses increase by 13 times. When the m index is increased as well, both x and y power losses increase, so the total mode-mismatch-induced power loss increases by 13 times.

Mode-mismatch-induced power losses in the OMC correspond directly to a loss of signal and increased quantum noise. Changing to an equivalently stable higher-order spatial mode will reduce thermal noise; however, unless the HOM matching is improved compared to the TEM00 mode matching, the mode-mismatching-induced signal degradation will be 13 times worse for a HG33 and 31 times worse for a HG55 carrier mode.

Acknowledgment. The authors jointly thank Dr. Chris Collins and Dr. Conor Mow-Lowry for helpful discussions.

Disclosures. The authors declare no conflicts of interest.

See Supplement 1 for supporting content.

REFERENCES

1. A. M. Yao and M. J. Padgett, Adv. Opt. Photon. **3**, 161 (2011).
2. D. Grier, Nature **424**, 810 (2003).
3. M. Mestre, B. F. Diry, V. de Lesegno, and L. Pruvost, Eur. Phys. J. D **57**, 87 (2010).
4. D. J. Richardson, J. M. Fini, and L. E. Nelson, Nat. Photonics **7**, 354 (2013).
5. LIGO Collaboration, Phys. Rev. Lett. **123**, 231107 (2019).
6. LIGO Collaboration, Classical Quantum Gravity **32**, 074001 (2015).
7. B. Mours, E. Tournefier, and J.-Y. Vinet, Classical Quantum Gravity **23**, 5777 (2006).
8. J.-Y. Vinet, Classical Quantum Gravity **24**, 3897 (2007).
9. S. Chelkowski, S. Hild, and A. Freise, Phys. Rev. D **79**, 122002 (2009).
10. S. Ast, S. Di Pace, J. Millo, M. Pichot, M. Turconi, and W. Chaibi, "Generation of very high-order high purity Gaussian modes via spatial light modulation," arXiv:1902.01671 (2019).
11. B. Sorazu, P. J. Fulda, B. W. Barr, A. S. Bell, C. Bond, L. Carbone, A. Freise, S. Hild, S. H. Huttner, J. Macarthur, and K. A. Strain, Classical Quantum Gravity **30**, 035004 (2013).
12. G. Vajente and R. A. Day, Phys. Rev. D **87**, 122005 (2013).
13. E. Schreiber, "Gravitational-wave detection beyond the quantum shot-noise limit," Ph.D. dissertation (Leibniz Universität Hannover, 2018).
14. LIGO Collaboration, Nat. Photonics **7**, 613 (2013).
15. A. Perreca, A. F. Brooks, J. W. Richardson, D. Töyrä, and R. Smith, Phys. Rev. D **101**, 102005 (2020).
16. A. Meurer, C. P. Smith, M. Paprocki, O. Čertík, S. B. Kirpichev, M. Rocklin, A. Kumar, S. Ivanov, J. K. Moore, S. Singh, T. Rathnayake, S. Vig, B. E. Granger, R. P. Muller, F. Bonazzi, H. Gupta, S. Vats, F. Johansson, F. Pedregosa, M. J. Curry, A. R. Terrel, V. Roučka, A. Saboo, I. Fernando, S. Kulal, R. Cimrman, and A. Scopatz, PeerJ Comput. Sci. **3**, e103 (2017).
17. A. Jones, "Impact and mitigation of wavefront distortions in precision interferometry (forthcoming)," Ph.D. dissertation (University of Birmingham, 2020).
18. F. Bayer-Helms, Appl. Opt. **23**, 1369 (1984).
19. C. Bond, D. Brown, A. Freise, and K. A. Strain, Living Rev. Relativ. **19**, 3 (2017).
20. A. W. Jones and A. Freise, "Increased sensitivity of higher-order laser beams to mode mismatches: supplemental code (figshare)," 2020, https://doi.org/10.6084/m9.figshare.12860984.
21. D. D. Brown, P. Jones, S. Rowlinson, A. Freise, S. Leavey, A. C. Green, and D. Toyra, "Pykat: python package for modelling precision optical interferometers," arXiv:2004.06270 (2020).
22. C. Bond, "How to stay in shape: overcoming beam and mirror distortions in advanced gravitational wave interferometers," Ph.D. dissertation (University of Birmingham, 2014).
23. A. Freise, G. Heinzel, H. Lück, R. Schilling, B. Willke, and K. Danzmann, Classical Quantum Gravity **21**, S1067 (2004).
24. D. D. Brown and A. Freise, "Finesse," 2014, http://www.gwoptics.org/finesse.